Close or connected: Distance and connectivity effects on transport in networks

V. Tejedor, O. Bénichou, and R. Voituriez
Laboratoire de Physique Théorique de la Matière Condensée, UMR CNRS/UPMC, Université Pierre et Marie Curie, 4 Place Jussieu, F-75255 Paris Cedex, France
(Received 22 February 2011; published 3 June 2011)

We develop an analytical approach that provides the dependence of the mean first-passage time (MFPT) for random walks on complex networks both on the target connectivity and on the source-target distance. Our approach puts forward two strongly different behaviors depending on the type—compact or non compact—of the random walk. In the case of non compact exploration, we show that the MFPT scales linearly with the inverse connectivity of the target and is largely independent of the starting point. On the contrary, in the compact case, the MFPT is controlled by the source-target distance, and we find that unexpectedly the target connectivity becomes irrelevant for remote targets.

DOI: 10.1103/PhysRevE.83.066102 PACS number(s): 89.75.Hc, 05.40.Fb

I. INTRODUCTION

Complex networks theory is nowadays a common tool to analyze a broad class of phenomena in social, biological, or physical sciences [1–3]. An important issue in the field is to quantify the impact of topological properties of a network on its transport properties. As a paradigm of transport process, random walks on complex networks have been intensely studied [4–9], and the mean first-passage time (MFPT) [10] to a target node—which quantifies the time needed for a random walker to find a target on the network—has been widely used as an indicator of transport efficiency [11–18].

A striking topological feature of many real-world complex networks is the wide distribution of the number k of links attached to a node—the connectivity—as exemplified by the now celebrated class of scale-free networks, such as internet [19], biological networks [20], stock markets [21] or urban traffic [22], for which the connectivity is distributed according to a power law. The impact of connectivity on transport properties has been put forward in [8,23–25], where it was found in different examples that transport toward a target node can be favored by a high connectivity of the target, and different functional forms of the dependence of the MFPT on the target connectivity were proposed. On the other hand, the dependence of the MFPT on geometric properties, such as the volume of the network and the source to target distance, has been obtained recently in [26–29], where it was shown that the starting position of the random walker plays a crucial role in the target search problem. In this context, quantifying the relative importance of distance and connectivity effects on transport properties on complex networks remains an important and widely unanswered question, which can be summarized as follows: is it faster for a random walker to find a close or a highly connected target?

Here we propose a general framework, applicable to a broad class of networks, which deciphers the dependence of the MFPT both on the target connectivity and on the source to target distance, and provides a global understanding of recent results obtained on specific examples. Our approach highlights two strongly different behaviors depending on the so-called type—compact or non compact—of the random walk. In the case of non compact exploration, the MFPT is found to scale linearly with the inverse connectivity of the target and to be widely independent of the starting point. On the contrary, in the compact case, the MFPT is controlled by the source to target distance, and we find that unexpectedly the target connectivity is irrelevant for remote targets. This analytical approach, validated numerically on various examples of networks, can be extended to other relevant first-passage observables, such as splitting probabilities or occupations times [27].

II. MODEL AND NOTATIONS

We are interested in the MFPT denoted $\overline{\mathbf{T}}(\mathbf{r}_T|\mathbf{r}_S)$ of a discrete Markovian random walker to a target $\mathbf{r}_T$, starting from a source point $\mathbf{r}_S$, and evolving in a network of N sites. We denote by $k(\mathbf{r})$ the connectivity (number of nearest neighbors) of site $\mathbf{r}$, and by $\langle k\rangle$ its average over all sites with a flat measure. The corresponding degree distribution is denoted by $p(k)$. We assume that at each time step n, the walker, at site $\mathbf{r}$, jumps to one of the neighboring sites with probability $1/k(\mathbf{r})$. Let $P(\mathbf{r},n|\mathbf{r}')$ be the propagator, i.e., the probability that the walker is at $\mathbf{r}$ after n steps, starting from $\mathbf{r}'$. The stationary probability distribution is then given by $P_{\rm stat}(\mathbf{r}) = k(\mathbf{r})/N\langle k\rangle$, and it can be shown that detailed balance yields the following symmetry relation:

$$P(\mathbf{r},n|\mathbf{r}')P_{\rm stat}(\mathbf{r}') = P(\mathbf{r}',n|\mathbf{r})P_{\rm stat}(\mathbf{r}), \tag{1}$$

which will prove to be useful.

We consider networks with only short-range degree correlations, namely such that $\langle k(\mathbf{r})k(\mathbf{r}')\rangle = \langle k\rangle^2$ for $|\mathbf{r}-\mathbf{r}'|$ larger than a cutoff distance R, where the average is taken over all pairs $\mathbf{r},\mathbf{r}'$ with $|\mathbf{r}-\mathbf{r}'|$ fixed. Here $|\mathbf{r}-\mathbf{r}'|$ denotes the chemical distance between $\mathbf{r}$ and $\mathbf{r}'$, defined as the length (in number of steps) of the shortest path between $\mathbf{r}$ and $\mathbf{r}'$. This hypothesis of short-range degree correlations is verified in particular by networks whose Pearson assortativity coefficient [30] is zero, such as Erdos-Renyi networks. It is, however, less restrictive, since local degree correlations can exist and many networks actually comply with this assumption, as exemplified below. The hypothesis of short-range degree correlations implies in particular that the degree distribution in a shell of radius $r > R$, defined as the set of sites $\mathbf{r}'$ such that $|\mathbf{r}-\mathbf{r}'| = r$, is identical

 ©2011 American Physical Society

to the degree distribution $p(k)$ over the whole network, so that

$$\sum_{\mathbf{r}'\setminus|\mathbf{r}-\mathbf{r}'|=r} P_{\rm stat}(\mathbf{r}') \simeq N_{\mathbf{r}}(r)/N, \tag{2}$$

where $N_{\mathbf{r}}(r)$ is the number of sites $\mathbf{r}'$ such that $|\mathbf{r}-\mathbf{r}'|=r$. We then introduce the weighted average at distance r of a function f of two space variables defined by

$$\{f(\mathbf{r},\mathbf{r}')\}_{\mathbf{r}'} = \frac{N}{N_{\mathbf{r}}(r)} \sum_{\mathbf{r}'/|\mathbf{r}-\mathbf{r}'|=r} f(\mathbf{r},\mathbf{r}')P_{\rm stat}(\mathbf{r}'), \tag{3}$$

and the standard flat average

$$\langle f(\mathbf{r},\mathbf{r}')\rangle_{\mathbf{r}'} = \frac{1}{N_{\mathbf{r}}(r)} \sum_{\mathbf{r}'/|\mathbf{r}-\mathbf{r}'|=r} f(\mathbf{r},\mathbf{r}'). \tag{4}$$

III. SCALING FORM OF THE PROPAGATOR FOR SCALE-INVARIANT PROCESSES

We focus hereafter on transport processes having scale-invariant properties. In this case, we can assume that the propagator in the infinite network size limit P_0, after averaging over points at a distance r from the starting point, satisfies the standard scaling for $|\mathbf{r}-\mathbf{r}'|>R$:

$$\langle P_0(\mathbf{r},n|\mathbf{r}')\rangle_{\mathbf{r}} \propto n^{-d_f/d_w}\,\Pi\left(\frac{r}{n^{1/d_w}}\right), \tag{5}$$

where the fractal dimension d_f characterizes the accessible volume $V_r \propto r^{d_f}$ within a sphere of radius r, and the walk dimension d_w characterizes the distance $r \propto n^{1/d_w}$ covered by a random walker in n steps. $\Pi(u)$ is a scaling function here, which for instance is well approximated by a stretched exponential [$\Pi(u)=\exp(-u^{\alpha})$] in the case of fractal media [31], where $\alpha>0$ depends on the medium. A first central result of this paper is to show numerically that the dependence of the propagator on the connectivity of the target site can be actually made explicit and reads

$$\langle P_0(\mathbf{r},n|\mathbf{r}')\rangle_{\mathbf{r},k} \propto k n^{-d_f/d_w}\,\Pi\left(\frac{r}{n^{1/d_w}}\right), \tag{6}$$

where the average is taken over sites $\mathbf{r}$ at a distance r from $\mathbf{r}'$ with fixed connectivity k. An argument supporting the k dependence hypothesized in Eq. (6) is that it satisfies the symmetry relation of Eq. (1). Numerical simulations on various examples of scale-invariant networks, such as percolation clusters and (u,v) flowers (see definition below), validate this assumption, as shown in Figs. 1 and 2. We stress that the scaling form (6) is verified in the cases of both compact ($d_w>d_f$) and non compact ($d_w<d_f$) exploration. We believe that this result on its own can be important in the analysis of transport processes on networks. We show next that it enables us to obtain the explicit dependence of first-passage properties on the connectivity of the target site.

IV. MEAN FIRST-PASSAGE TIME

We now extend the theory developed in [26] to compute the MFPT of a discrete Markovian random walker to a target $\mathbf{r}_T$, and obtain explicitly its dependence on $k(\mathbf{r}_T)$. As shown

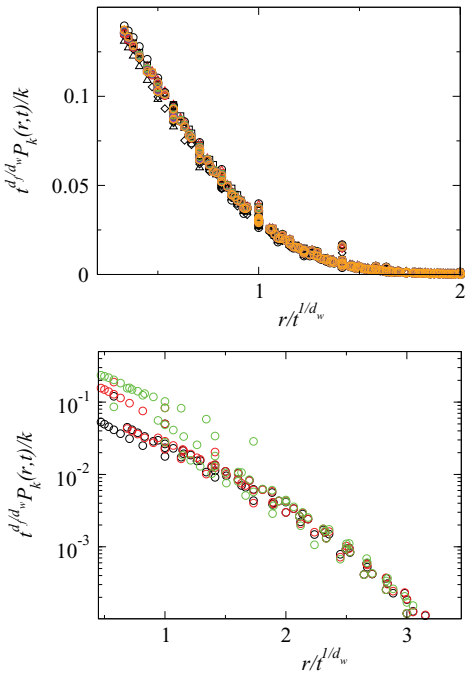

FIG. 1. (Color online) Plot of the propagator $P(\mathbf{r}_T,n|\mathbf{r}_S)$ for non compact exploration. Top: Supercritical 3D percolation networks ($p=0.8$) of different sizes and for different $k(\mathbf{r}_T)$. $\mathbf{r}_s$ is chosen in the center of the network, and t is small enough to avoid hits on the network's border. Here r denotes the usual Euclidean distance. Black, red, green, blue, magenta, and orange symbols stand respectively for $k=1$, 2, 3, 4, 5, and 6. Circles, triangles, diamonds, and squares stand respectively for networks of size 20^3, 25^3, 30^3, and 40^3. Bottom: (2,2,2) flowers. Black, red, and green circles stand respectively for $k=2$, 6, and 18.

explicitly in [26,33] (see also [4] for a different derivation), the MFPT satisfies the following exact expression:

$$P_{\rm stat}(\mathbf{r}_T)\overline{\mathbf{T}}(\mathbf{r}_T|\mathbf{r}_S) = H(\mathbf{r}_T|\mathbf{r}_T) - H(\mathbf{r}_T|\mathbf{r}_S), \tag{7}$$

where $H(\mathbf{r}|\mathbf{r}')=\sum_{n=1}^{\infty}[P(\mathbf{r},n|\mathbf{r}')-P_{\rm stat}(\mathbf{r})]$ is the pseudo-Green function of the problem [34]. Note that averaging Eq. (7) for $\mathbf{r}_S$ covering the nearest neighbors of $\mathbf{r}_T$ gives the expression of the averaged MFPT $\langle\overline{\mathbf{T}}\rangle_{\rm Kac}(\mathbf{r}_T)$ expected from the Kac formula [35,36]:

$$\langle\overline{\mathbf{T}}\rangle_{\rm Kac}(\mathbf{r}_T) = 1/P_{\rm stat}(\mathbf{r}_T) - 1 = N\langle k\rangle/k(\mathbf{r}_T) - 1, \tag{8}$$

which we will use below.

Following [26], we consider the large N limit of Eq. (7). Making use of Eq. (1), we obtain

$$P_{\rm stat}(\mathbf{r}_T)\overline{\mathbf{T}}(\mathbf{r}_T|\mathbf{r}_S) \sim G_0(\mathbf{r}_T|\mathbf{r}_T) - \frac{k(\mathbf{r}_T)}{k(\mathbf{r}_S)}G_0(\mathbf{r}_S|\mathbf{r}_T). \tag{9}$$

Here G_0 is the usual infinite space Green function defined by $G_0(\mathbf{r}|\mathbf{r}')=\sum_{n=1}^{\infty}P_0(\mathbf{r},n|\mathbf{r}')$, and $\sim$ denotes equivalence for large N. It is useful to notice that this leading term of the MFPT still satisfies the Kac formula (8). We next take the weighted average of Eq. (9) over the source points and obtain

$$P_{\rm stat}(\mathbf{r}_T)\overline{\mathbf{T}}_{\mathbf{r}_T}(r) \sim G_0(\mathbf{r}_T|\mathbf{r}_T) - \frac{k(\mathbf{r}_T)}{\langle k\rangle}\langle G_0(\mathbf{r}_S|\mathbf{r}_T)\rangle_{\mathbf{r}_S}, \tag{10}$$

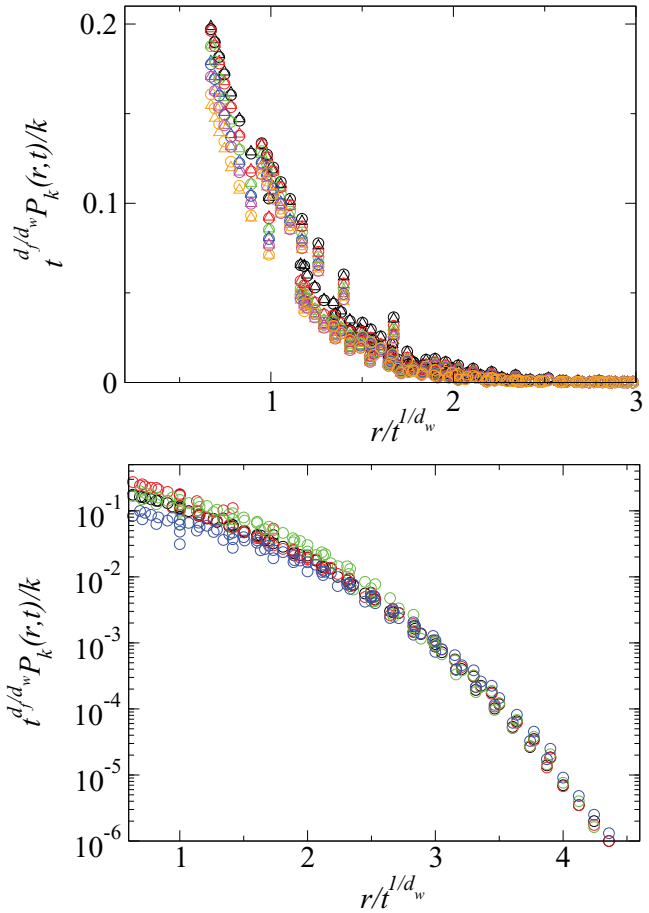

FIG. 2. (Color online) Plot of the propagator $P(\mathbf{r}_T,n|\mathbf{r}_S)$ for compact exploration.Top: Critical 3D percolation networks ($p = 0.2488$) of different sizes and for different $k(\mathbf{r}_T)$. r_s is chosen in the center of the network, and t is small enough to avoid hits on the network's border. Black, red, green, blue, magenta, and orange symbols stand respectively for $k = 1$, 2, 3, 4, 5, and 6. Circles and triangles stand respectively for networks of size 40^3 and 50^3. Bottom: (3,3) flowers (see [32]) for different $k(\mathbf{r}_T)$. Black, red, green, and blue circles stand respectively for $k = 2$, 4, 8, and 16.

where we defined $\overline{\mathbf{T}}_{\mathbf{r}_T}(r) \equiv \{\overline{\mathbf{T}}(\mathbf{r}_T|\mathbf{r}_S)\}_{\mathbf{r}_S}$. Substituting the scaling (5) in Eq. (10) then yields the large N equivalence of the MFPT to a target site $\mathbf{r}_T$ averaged over sources, which is valid for $r > R$:

$$\overline{\mathbf{T}}_{\mathbf{r}_T}(r) \sim N\langle k\rangle(A_k + Br^{d_w-d_f}). \tag{11}$$

In this expression, the constant A_k depends on the connectivity k of the target and B is a constant independent of k and r, which depends on the scaling function Π. We now distinguish two regimes depending on the compact or non compact nature of the transport process, and focus on the large r regime.

A. Compact case $d_w \geqslant d_f$

In the compact case $d_w \geqslant d_f$, which corresponds to recurrent random walks, we obtain that the MFPT scales in the large r limit as

$$\overline{\mathbf{T}}_{\mathbf{r}_T}(r) \sim N\langle k\rangle Br^{d_w-d_f}. \tag{12}$$

This shows that, unexpectedly, the MFPT is asymptotically independent of the connectivity of the target, while the dependence on the distance r is crucial. Equation (11) is valid for r large enough (typically $r > R$). The dependence of A_k on k, which impacts on the MFPT for r small only, can be estimated by assuming that this expression still holds approximately for short distances. Following [37], we take $r = 1$ in Eq. (11) and use the Kac formula (8) to obtain

$$1/k \approx A_k + B, \tag{13}$$

which provides the k dependence of A_k. We next aim at evaluating B. We introduce the weighted average of the MFPT over the target point $\tau(r) = \sum_{\mathbf{r}_T} P_{\text{stat}}(\mathbf{r}_T)\overline{\mathbf{T}}_{\mathbf{r}_T}(r)$. Using Eq. (13), this quantity writes

$$\tau(r) \sim N\left[1 + B\langle k\rangle(r^{d_w-d_f} - 1)\right]. \tag{14}$$

In the case of compact exploration, the continuous space limit can be defined (see [37]) and imposes $\tau(r \to 0) = 0$. This extra equation, based on the existence of a continuous limit, enables us to evaluate B as $B = 1/\langle k\rangle$. Note that, for fractal trees ($d_w - d_f = 1$), we recover the exact result $\tau(r) = Nr$. Finally, one has

$$\overline{\mathbf{T}}_{\mathbf{r}_T}(r) \sim N\langle k\rangle\left(\frac{1}{k} + \frac{1}{\langle k\rangle}(r^{d_w-d_f} - 1)\right), \tag{15}$$

which fully elucidates the dependence of the MFPT on k and r. We recall here that this expression is originally derived for r large, and that the small r regime relies on the less controlled assumption that the scaling form of the propagator (6) holds for any distance r and, in particular, that a continuous limit exists. It will, however, prove numerically to be accurate in various examples for all r values.

B. Non compact case $d_w < d_f$

In the non compact (or transient) case $d_w < d_f$, we obtain that the MFPT scales in the large r limit as

$$\overline{\mathbf{T}}_{\mathbf{r}_T}(r) \sim N\langle k\rangle A_k. \tag{16}$$

This shows that the MFPT is independent of r for r large, as was already discussed in the literature [26]. The dependence on k is now fully contained in the constant A_k, which we now determine. Following [24], we assume that the FPT distribution is proportional to $\exp[-Akt/(N\langle k\rangle)]$, with $A = O(1)$, and widely independent of r in agreement with the result obtained in Eq. (16) for the first moment. This implies that the global MFPT, defined as the MFPT averaged over all source points and denoted by $\{\overline{\mathbf{T}}_{\mathbf{r}_T}\}$, scales as $\{\overline{\mathbf{T}}_{\mathbf{r}_T}\} \propto N\langle k\rangle/k$. Using the exact result derived in [25]

$$\{\overline{\mathbf{T}}_{\mathbf{r}_T}\} = \frac{H(\mathbf{r}_T|\mathbf{r}_T)}{P_{\text{stat}}(\mathbf{r}_T)}, \tag{17}$$

we obtain that $H(\mathbf{r}_T|\mathbf{r}_T)$, and therefore asymptotically the infinite space Green function $G_0(\mathbf{r}_T|\mathbf{r}_T)$, is independent of k in the case of non compact exploration. This is checked numerically in Fig. 3. Identifying in Eq. (11) $A_k = G_0(\mathbf{r}_T|\mathbf{r}_T)/k$, which is finite in the case of non compact exploration, we finally obtain

$$\overline{\mathbf{T}}_{\mathbf{r}_T}(r) \sim N\langle k\rangle\left(\frac{A}{k} - Br^{d_w-d_f}\right). \tag{18}$$

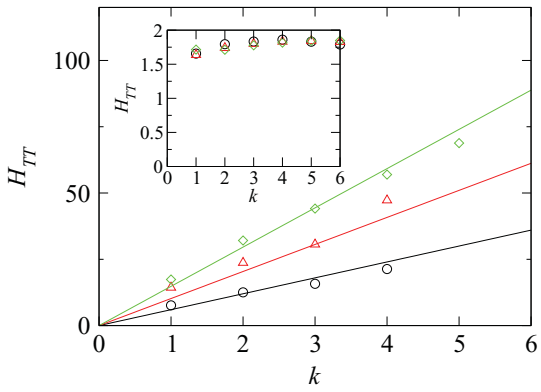

FIG. 3. (Color online) Numerical computation of $H(\mathbf{r}_T|\mathbf{r}_T)$ averaged over a network of a given size, as a function of the target connectivity k, on supercritical ($p = 0.8$) and critical ($p = 0.2488$) 3D percolation networks. The inset stands for the supercritical percolation network, for three sizes 10^3 (black circles), 15^3 (red triangles), and 20^3 (green diamonds). Equation (22) gives $H(\mathbf{r}_T|\mathbf{r}_T) = C$. The main figure stands for the critical percolation network, also for three sizes (same symbols), and a fit in CkN^{d_w/d_f-1} (straight line).

As in the compact case, this expression is valid for r large and becomes hypothetical for r small. It reveals that, in the case of non compact exploration, the MFPT is independent of r for r large and scales as the inverse connectivity of the target. This behavior is in strong contrast with the case of compact exploration.

V. SUMMARY OF THE RESULTS AND DISCUSSION

Finally, our central result can be summarized as follows, where the case of marginal exploration ($d_w = d_f$) has been obtained along the same line:

$$\frac{\overline{\mathbf{T}}_{\mathbf{r}_T}(r)}{N\langle k\rangle} \sim \begin{cases} \dfrac{1}{k} + \dfrac{1}{\langle k\rangle}\left(r^{d_w-d_f} - 1\right) & \text{if } d_w > d_f, \\ \dfrac{1}{k} + B\,\ln(r) & \text{if } d_w = d_f, \\ \dfrac{A}{k} - Br^{d_w-d_f} & \text{if } d_w < d_f. \end{cases} \tag{19}$$

This expression is very general and shows the respective impact of distance and connectivity on the MFPT. In particular, the MFPT is fully explicitly determined in the compact case. The positive constants A and B depend on the network in the case of non compact exploration. We comment that in both cases the target connectivity k plays an important role at short distances r. However, for large source-target distances r, the k dependence is damped out in the compact case, while it remains important in the non compact case. The r dependence is found to be important in the compact case and largely irrelevant in the non compact case in agreement with previous results [26]. The question raised in the Introduction can therefore be answered as follows: in the non compact case connected targets are found the fastest almost independently of their distance, while in the compact case close targets are found the fastest almost independently of their connectivity.

We can conclude that for self-similar networks with short-range degree correlations, the main criterion that governs the behavior of $\overline{\mathbf{T}}$ is the type (compact or non compact) of the random walk. In particular, the existence of loops is irrelevant. Further comments are in order. (i) As stressed above, Eq. (19) is derived in the large r regime. Its applicability to the small r regime relies on the assumption that the scaling form of the propagator (6) holds for all values of r, which is not always satisfied for real networks. In particular, when degree correlations exist, the relation $B = 1/\langle k\rangle$ obtained in the compact case gives only a rough estimate and the result of Eq. (19) is valid only for r larger than the correlation length. (ii) Our results can be extended to the case of non-self-similar networks, still under the assumption that degree correlations are negligible. Following the method developed above, one can infer that

$$\overline{\mathbf{T}}_{\mathbf{r}_T}(r) \sim N\langle k\rangle[A/k + g(r)], \tag{20}$$

where g does not depend on k and satifies $g(r \to \infty) = C$ in the transient case and $g(r \to \infty) = \infty$ in the recurrent case. The relative impact of connectivity and distance is therefore qualitatively the same as in the case of self-similar networks discussed above. (iii) Incidentally, our results straightforwardly yield the k dependence of the MFPT averaged over all source points (global MFPT). We find, in the large N limit,

$$\{\overline{\mathbf{T}}_{\mathbf{r}_T}\} \sim \begin{cases} CN^{d_w/d_f} & \text{if } d_w > d_f, \\ CN\,\ln N & \text{if } d_w = d_f, \\ CN/k & \text{if } d_w < d_f, \end{cases} \tag{21}$$

which complements previous results obtained in [25]. This expression, along with Eq. (17), yields as a by-product the large N asymptotics of $H(\mathbf{r}_T|\mathbf{r}_T)$:

$$H(\mathbf{r}_T|\mathbf{r}_T) \sim \begin{cases} CkN^{d_w/d_f-1} & \text{if } d_w > d_f, \\ Ck\,\ln N & \text{if } d_w = d_f, \\ C & \text{if } d_w < d_f. \end{cases} \tag{22}$$

This k dependence of $H(\mathbf{r}_T|\mathbf{r}_T)$ is checked numerically in Fig. 3 and directly validates the k dependence of the global MFPT.

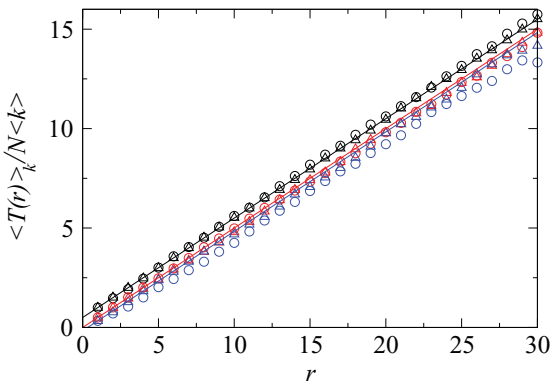

FIG. 4. (Color online) Mean first passage time $[\langle\overline{\mathbf{T}}_{\mathbf{r}_T}(r)\rangle_k]$ for critical Erdos-Renyi networks, as a function of the source-target distance r, for a various target connectivity k ($k = 1$, 2, and 3 from top to bottom). Circles and triangles stand for simulation results, for two sizes of the network (1000 and 2000 nodes); straight lines stand for the zero-constant formula ($\langle k\rangle = 2$) of Eq. (19).

VI. NUMERICAL SIMULATIONS

We have checked our main result (19) on various examples of networks, corresponding to compact or non compact random walks as detailed below. We stress that the zero constant formula obtained in the compact case is in good agreement with numerical simulations in all the examples that we have considered. As explained in Sec. V, our results rely on a scaling hypothesis of the propagator that is not fully satisfied for small r; we therefore expect a good agreement only for r large enough, as is indeed observed.

Erdos-Renyi networks. Erdos-Renyi networks can be defined as a percolation cluster on a complete graph: for every pair of nodes (i,j), a link exists with probability p. The network is then defined as the largest cluster. We considered clusters at the percolation transition obtained for $p = 1/N$, for which the estimated d_f is 1.9–2.0 [38]. We computed numerically $d_w \simeq 2.9$, which shows that exploration is compact. Numerical results of Fig. 4 are in very good agreement with the scaling (19).

(u,v) flowers. These networks are constructed recursively as described in [32]: at each step, every link is substituted by two paths of length u and v. We extended this definition to (u,v,w) flowers, for which a third path is added. For those networks, $d_w - d_f = -\ln(1/u + 1/v + 1/w)/\ln(u)$ (if $1 < u \leqslant v \leqslant w$). Figure 5 shows a very good agreement of numerical simulations with Eq. (19), despite the small size of the networks.

Random flowers. These networks are constructed recursively as described in [39]: at each step, every link is substituted by two paths of length u and v. d_f and d_w are determined numerically for those networks; in our example, (2,2)-random flowers are compact networks ($d_w - d_f \simeq 0.6$). Figure 5 shows a good agreement of numerical simulations with Eq. (19).

Networks of Kozma et al. These networks, defined in [40], are simple Euclidian lattices in which long-range links ("shortcuts") are added. A shortcut starts from each node with probability p and leads to a node at a distance r, where r is distributed according to a power law of index α. We consider here a one-dimensional (1D) Euclidian lattice. Exploration is

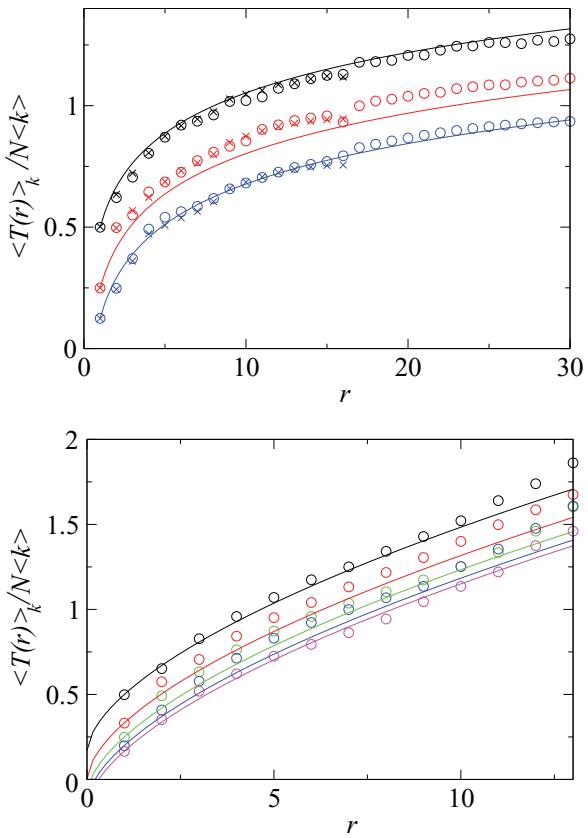

FIG. 5. (Color online) Mean first passage time $[\langle \overline{\mathbf{T}}_{\mathbf{r}_T}(r)\rangle_k]$ as a function of the source-target distance r, for a various target connectivity k. Top: (2,2) flowers ($d_w = d_f$). Circles and triangles stand for simulation results, for two sizes of the network (generations 4 and 5); straight lines stand for the formula $1/k + B\ \ln(r)$ of Eq. (19), with $B = 0.24$. $k = 2,4,8$ from top to bottom. Bottom: random (2,2) flowers ($d_w = 2.5$ and $d_f = 1.9$). Circles stand for simulation results; straight lines stand for $1/k + 1/\langle k\rangle (r^{d_w - d_f})$ ($\langle k\rangle = 3$) of Eq. (19). $k = 2,3,4,5,6$ from top to bottom.

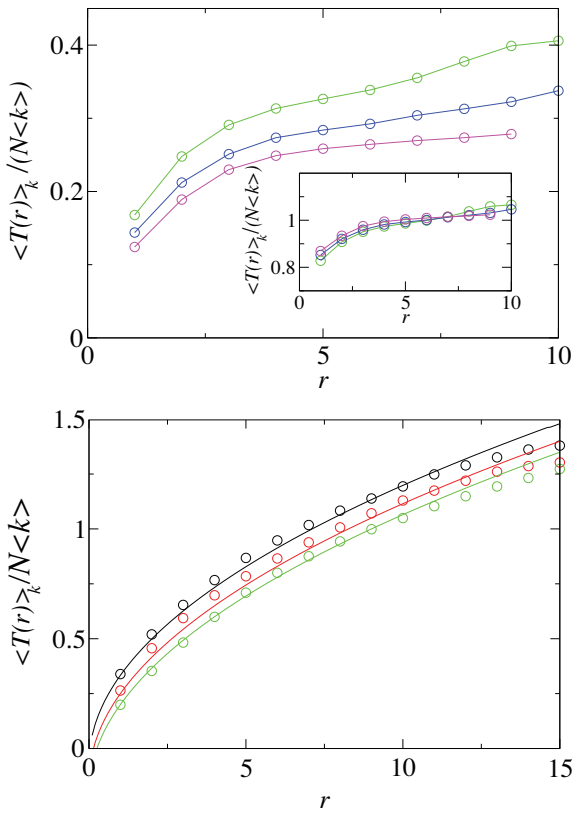

FIG. 6. (Color online) Mean first passage time $[\langle \overline{\mathbf{T}}_{\mathbf{r}_T}(r)\rangle_k]$ as a function of the source-target distance r, for a various target connectivity k. Top: non compact Kozma network of size $X = 400$, $\alpha = 1.0$. The inset shows a translation along the y axis of A/k with $A = 2.04$ according to Eq. (20). As predicted, this quantity does not depend on k. Here $k = 6,7,8$ from top to bottom. Bottom: compact Kozma network of size $X = 50$, $\alpha = 2.5$. The expected scaling is in $r^{0.5}$: circles stand for simulation results; straight lines stand for $1/k + 1/\langle k\rangle (r^{0.5} - 1)$ ($\langle k\rangle = 2.5$) of Eq. (19). Here $k = 3,4,5$ from top to bottom.

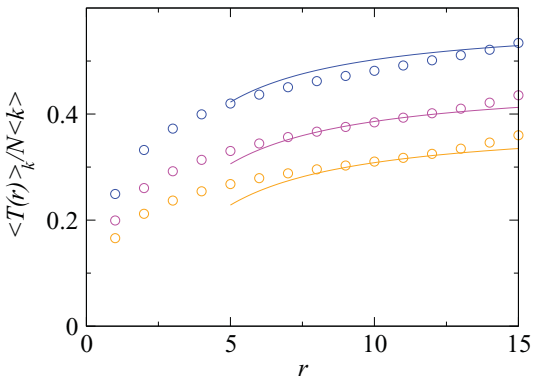

FIG. 7. (Color online) Mean first passage time $[\langle \overline{\mathbf{T}}_{\mathbf{r}_T}(r)\rangle_k]$ as a function of the source-target distance r, for a various target connectivity k, on a supercritical 3D percolation network ($p = 0.8$). For this network, $d_w \simeq 2$ and $d_f = 3$, the exploration is non compact. Circles stand for simulations results; straight lines stand for a fit by $A/k + Br^{d_w - d_f}$, with $A \simeq 2.33$ and $B \simeq 0.8$. Here r denotes the usual Euclidean distance and $k = 4,5,6$ from top to bottom.

then compact for $\alpha > 2$ and non compact for $\alpha < 2$. Again, Fig. 6 shows a very good agreement of numerical simulations with Eq. (19).

Percolation clusters. We consider percolation clusters in the case of bond percolation in 3D cubic lattices. The critical probability is $p_c = 0.2488\ldots$ and one has $d_w = 3.88\ldots$ and $d_f = 2.58\ldots$ at criticality. If $p > p_c$, $d_f = 3$ (Euclidian dimension) and $d_w = 2$. Figure 7 shows a good agreement of numerical simulations with Eq. (19).

VII. CONCLUSION

To conclude, we have proposed a general theoretical framework that elucidates the connectivity and source-target distance dependence of the MFPT for random walks on networks. This approach leads to explicit solutions for self-similar networks and highlights two strongly different behaviors depending on the type—compact or non compact—of the random walk. In the case of non compact exploration, the MFPT is found to scale as the inverse connectivity of the target, and to be widely independent of the source-target distance. On the contrary, in the compact case, the MFPT is controlled by the source-target distance and we find that, unexpectedly, the target connectivity is irrelevant for remote targets. The question raised in the Introduction can therefore be answered as follows: in the non compact case, connected targets are found the fastest almost independently of their position, while in the compact case close targets are found the fastest almost independently of their connectivity. Last, we stress that, following [27], this explicit determination of MFPTs can be straightforwardly generalized to obtain other relevant first-passage observables, such as splitting probabilities or occupation times.

ACKNOWLEDGMENTS

V.T. wishes to thank Dr. Hakim Lakmini for useful discussions.

[1] R. Albert and A.-L. Barabasi, Rev. Mod. Phys. **74**, 47 (2002).
[2] S. N. Dorogovtsev, A. V. Goltsev, and J. F. F. Mendes, Rev. Mod. Phys. **80**, 1275 (2008).
[3] A. Barrat, M. Barthélémy, and A. Vespignani, *Dynamical Processes in Complex Networks* (Cambridge University Press, New York, 2008).
[4] J. D. Noh and H. Rieger, Phys. Rev. Lett. **92**, 118701 (2004).
[5] E. M. Bollt and D. ben Avraham, New J. Phys. **7**, 26 (2005).
[6] S. Nechaev and R. Voituriez, J. Phys. A **36**, 43 (2003); **34**, 11069 (2001).
[7] A. N. Samukhin, S. N. Dorogovtsev, and J. F. F. Mendes, Phys. Rev. E **77**, 036115 (2008).
[8] A. Baronchelli, M. Catanzaro, and R. Pastor-Satorras, Phys. Rev. E **78**, 011114 (2008).
[9] M. Kitsak, L. K. Gallos, S. Havlin, F. Liljeros, L. Muchnik, H. E. Stanley, and H. A. Makse, Nat. Phys. **6**, 888 (2010).
[10] S. Redner, *A Guide to First Passage Time Processes* (Cambridge University Press, Cambridge, England, 2001).
[11] Z. G. Huang, X. J. Xu, Z. X. Wu, and Y. H. Wang, Eur. Phys. J. B **51**, 549 (2006).
[12] L. K. Gallos, C. Song, S. Havlin, and H. A. Makse, Proc. Natl. Acad. Sci. **104**, 7746 (2007).
[13] J. J. Kozak and V. Balakrishnan, Phys. Rev. E **65**, 021105 (2002).
[14] C. P. Haynes and A. P. Roberts, Phys. Rev. E **78**, 041111 (2008).
[15] E. Agliari, Phys. Rev. E **77**, 011128 (2008).
[16] E. Agliari and R. Burioni, Phys. Rev. E **80**, 031125 (2009).
[17] Z. Zhang, Y. Qi, S. Zhou, W. Xie, and J. Guan, Phys. Rev. E **79**, 021127 (2009).
[18] Z. Zhang, S. Zhou, W. Xie, L. Chen, Y. Lin, and J. Guan, Phys. Rev. E **79**, 061113 (2009).
[19] M. Faloutsos, P. Faloutsos, and C. Faloutsos, in *SIGCOMM '99: Proceedings of the Conference on Applications, Technologies, Architectures, and Protocols for Computer Communication* (ACM, New York, 1999), pp. 251–262.
[20] V. van Noort, B. Snel, and M. Huynen, EMBO Rep. **5**, 280 (2004).
[21] H. Kim, I. Kim, Y. Lee, and B. Kahng, *7th International Workshop on Similarity in Diversity, Tokyo, Japan, 2001* [J. Korean Phys. Soc. **40**, 1105 (2002)].
[22] J. Wu, Z. Gao, H. Sun, and H. Huang, Mod. Phys. Lett. B **18**, 1043 (2004).
[23] E. López, S. V. Buldyrev, S. Havlin, and H. E. Stanley, Phys. Rev. Lett. **94**, 248701 (2005).
[24] A. Kittas, S. Carmi, S. Havlin, and P. Argyrakis, Europhys. Lett. **84**, 40008 (2008).
[25] V. Tejedor, O. Bénichou, and R. Voituriez, Phys. Rev. E **80**, 065104 (2009).
[26] S. Condamin, O. Benichou, V. Tejedor, R. Voituriez, and J. Klafter, Nature (London) **450**, 77 (2007).

[27] S. Condamin, V. Tejedor, R. Voituriez, O. Benichou, and J. Klafter, Proc. Natl. Acad. Sci. **105**, 5675 (2008).
[28] O. Benichou and R. Voituriez, Phys. Rev. Lett. **100**, 168105 (2008).
[29] O. Bénichou, C. Chevalier, J. Klafter, B. Meyer, and R. Voituriez, Nat. Chem. **2**, 472 (2010).
[30] M. E. J. Newman, Phys. Rev. Lett. **89**, 208701 (2002).
[31] D. Ben-Avraham and S. Havlin, *Diffusion and Reaction in Fractals and Disorders Systems* (Cambridge University Press, Cambridge, England, 2000).
[32] H. D. Rozenfeld, S. Havlin, and D. ben Avraham, New J. Phys. **9**, 175 (2007).
[33] S. Condamin, O. Benichou, and M. Moreau, Phys. Rev. Lett. **95**, 260601 (2005).
[34] G. Barton, *Elements of Green's Functions and Propagation* (Oxford Science Publications, New York, 1989).
[35] D. Aldous and J. Fill, *Reversible Markov Chains and Random Walks on Graphs* (1999) [http://www.stat.berkeley.edu/users/aldous/RWG/book.html].
[36] S. Condamin, O. Benichou, and M. Moreau, Phys. Rev. E **75**, 021111 (2007).
[37] O. Benichou, B. Meyer, V. Tejedor, and R. Voituriez, Phys. Rev. Lett. **101**, 130601 (2008).
[38] C. Song, L. K. Gallos, S. Havlin, and H. A. Makse, J. Stat. Mech.: Theory Exp. (2007) P03006.
[39] L. Tian and D.-N. Shi, Europhys. Lett. **84**, 58001 (2008).
[40] B. Kozma, M. B. Hastings, and G. Korniss, Phys. Rev. Lett. **95**, 018701 (2005).